Journal of Chemistry and Nutritional Biochemistry
https://jcnb.sabapub.com
E ISSN: 2709-5932

2026 Volume 7, Issue 1: 1–19

DOI: https://doi.org/10.48185/jcnb.v7i1.1969

Identification and Characterisation of Antimicrobial and Antioxidant Compounds in *Corchorus olitorius* Leaves: An LC-MS Analysis

Aziz Alans[1], Abdulfatah A. A. Saifan[*,2], Amat Al-Qader F. Al-Anesi[3], Vandana Hivrale[3], Deepak D. Kayande[1]

[1]S.B.E.S. College of Science, Aurangabad, Maharashtra, India-431004.
[2]School of Chemical Sciences, S.R.T.M. University, Nanded-431606.
[3]Department of Biochemistry, Dr. Babasaheb Ambedkar Marathwada University, Aurangabad-431001.
***Corresponding author: Abdulfatah A. A. Saifan. Email: abdulfatahsaifan123@gmail.com**

Received: 12.01.2026 • Accepted: 05.05.2026 • Published: 09.06.2026 • Final Version: 30.06.2025

Abstract: This study aimed to evaluate the phytochemical content and biological activities (antibacterial and antioxidant) of a methanol extract from the leaves of *Corchorus olitorius L*. The methanol extract was shown to be amenable to LC-MS testing. The extract was also subjected to in vitro tests for antibacterial and antioxidant properties. The 96 peaks in the LC-MS analysis indicate 96 distinct phytochemicals in the methanolic extract. The methanolic extract exhibited significant antibacterial activity against *E. coli*, with a minimum inhibitory concentration (MIC) of 125 µg/mL. In DPPH experiments, a strong antioxidant response was demonstrated. This article provides key diagnostic characteristics for the species Corchorus olitorius.

Keywords: Phytochemicals, *Corchorus olitorius*, LC-MS, Molecular docking, antibacterial activity, antioxidant activity

1. Introduction

Plant-based medicine has long been a staple of humankind. Since natural commodities have long been used to heal illnesses, it is important to search for new therapeutic medications from these plants (Aziziaram et al., 2021). Varieties of phytochemical compounds that plants contain each affect human physiology differently. The phytochemical screening approach can be used to identify these plant-based compounds that may serve as the building blocks for novel medications (Ezeonu & Ejikeme, 2016). A decrease in the discovery of new antimicrobial medicines is being accompanied by an increase in bacterial resistance to synthetic antibiotics. A focus shift has been made towards developing novel, effective, and affordable drugs to treat common microbial infections in order to combat these infections. This is especially important in developing nations where infectious diseases account for half of hospital deaths. Plant metabolism results in the production of compounds known as phytochemicals (Elisha et al., 2017). Numerous diseases are largely caused by free radicals; the body is able to generate reactive oxygen species (ROS) through the use of redox enzymes. Under normal conditions, chemical reactions with outside materials would continuously produce these ROS. Antioxidants help the body eliminate ROS under normal circumstances, balancing the ratio of ROS production to antioxidant availability. Oxidative stress arises when the frequency of reactive

* Corresponding Author: abdulfatahsaifan123@gmail.com

oxygen species (ROS) production exceeds that of antioxidants. In addition to causing inflammation and abnormal cell division, this stress can hasten the aging process and lead to several other health issues (Al-Hamoud et al., 2022).

Through the neutralization of oxidation in readily oxidizable substrates, antioxidants can scavenge free radicals (Sharma et al., 2020). This lessens the likelihood that free radicals will form. The kingdom of plants is abundant in antioxidants, including tocopherols, terpenoids, polyphenols, and ascorbate. They help the body's defences against oxidative stress brought on by free radicals. As people age, their bodies' effective defences are weakened. Therefore, it is crucial to offer individuals items that are rich in antioxidants. Such free radicals significantly degrade biomolecules such as deoxyribonucleic acids, amino acid chains, and fatty acids (Wadood et al., 2013).

Corchorus olitorius L., commonly called jute mallow, is a member of the genus *Corchorus* and the family Tiliaceae (Marwa et al., 2022). It has a lengthy history of use as a medicinal herb throughout the world. In agricultural regions, the vegetable is accepted as an invasive species and is also grown from seed. Its simple, deeply indented leaves and tiny yellow blooms with five petals distinguish this plant. Vitamins A, B1, B2, C, and E, fibre, and minerals such as calcium and iron are all abundant in the vegetable. Various tribes have used *C. olitorius* for traditional medical purposes, including treating tumours, measles, typhoid fever, malaria, gonorrhea, heart failure, stomach ulcers, and common colds. The vegetable is high in antioxidants (Marwa et al., 2022; Kundu et al., 2012; Giro & Ferrante, 2016; Islam, 2013; Saifan & Al-horaibi, 2021). The purpose of this study is to use LC-MS analysis to examine the phytochemical composition, antibacterial activity, and antioxidant potential of the methanol extract of *Corchorus olitorius*, including its anti-inflammatory, anti-carcinogenic, and antidiabetic qualities.

2. Materials and Methods

2.1. Preparation of Extract

The validated *Corchorus olitorius* leaves were cleaned, dried in the shade, powdered, and sealed in a container. Fifty mg of dried plant powder was extracted with 500 mL of 95% methanol in a Soxhlet apparatus. The extraction cycle was run until it lost all colour, which required more than 30 cycles. After the solvent was removed using a rotary vacuum evaporator, the liquid was cooled to ambient temperature, dried, and finally stored in an amber container under refrigeration. The plant was collected from the Himayat Bagh Area, Aurangabad, Maharashtra, India, in September 2019.

2.2. Evaluation of Analytical Properties

2.2.1 Liquid Chromatography–Mass Spectrometry (LC-MS)

To find the active phytoconstituents in the sample's methanol extract, an LC-ESI-Q-TOF MS system (Agilent Technologies 6550 I-funnel) was employed at SAIF, IIT, Bombay. The gradient system for the two-solvent elution method consists of 90% Acetonitrile + 10% Water + 0.1% Formic acid (B) and 0.1% Formic acid in water (A) at a flow rate of 0.3 mL/min and an injection volume of 5 µl. The gradient system began with 95% A and 5% B, reached 0% A:100% B at 25 minutes, then returned to the starting composition of 95% A and 5% B in 1 minute. It was then kept at that composition for 5 minutes. The chemicals channelled through the i-funnel Q-TOF were ionised in the dual positive (+ve) and negative (−ve) ESI modes for MS analysis. Capillary voltage 3500 V, mass range 120–1000 m/z, gas flow 13 L/min, gas temperature 250°C, sheath gas temperature 250°C, sheath gas flow 11, nebulizing gas pressure 35 psig, skimmer 65 V, fragmentor 175 V, and RF peak 750 V were the

settings used in the Q-TOF MS source. Using high-definition MS and MS/MS, the Mass Hunter software was used to profile, characterise, identify, and quantify the chemicals in the extract. The putative substances included in the sample were discovered by comparing the received analyzed samples with the Metlin database (Alrabie et al., 2023a).

2.3. Evaluation of Biological Properties

2.3.1 Antibacterial Activity

The broth-dilution method was used to find the MIC (Minimum Inhibitory Concentration) of a methanol extract of *Corchorus olitorius* leaves. Gram-positive strains of *Staphylococcus aureus* (MTCC96) and *Streptococcus pyogenes* (MTCC442), as well as *Escherichia coli* (MTCC443) and *Pseudomonas aeruginosa* (MTCC1688), were acquired from Microcare Laboratory in Surat. The control tube was incubated at 37°C for the entire night after being sub-cultured with a medium that supports the test microorganism's development. A stock solution of the extract and medication was prepared. Serial dilutions were made for the extract's primary and secondary evaluation. The extract's concentrations of 1000 µg/mL, 500 µg/mL, and 250 µg/mL were employed in the initial assessment. A secondary evaluation against microorganisms was conducted using the extract proven to be active in the primary evaluation. Secondary evaluation involved diluting the active extract to achieve concentrations of 200 µg/mL, 100 µg/mL, 50 µg/mL, 25 µg/mL, 12.5 µg/mL, and 6.25 µg/mL. To ensure that the extract concentration is reliable, the control microorganism's Minimum Inhibitory Concentration is noted. The MIC is the lowest concentration that exhibits a minimum of 99% inhibitory zone (Ola et al., 2016; Samreen et al., 2018).

2.3.2 Antioxidant Property

We used 1,1-diphenyl-2-picrylhydrazyl (DPPH) to assess the extract's antioxidant properties. Using a slightly modified spectrophotometric approach, DPPH scavenging activity was measured (Murshed, F and Al-kufl, D., 2024). Before adding 200 µM DPPH (prepared in 95% ethanol), 0.05 mL of extract dissolved in DMSO was diluted to 1.0 mL with ethanol to reach concentrations of 10–50 µg/mL. Equal parts of DMSO and ethanol were applied to the control. Every test was conducted using aliquots in triplicate. After 20 minutes of dark incubation, the spectrophotometer (Shimadzu UV-1800) was used to measure the drop in absorbance of test substances at 515 nm. The percentage inhibition was then computed using the following formula:

$$\% \text{ Scavenging} = [(A - B) / A] \times 100$$

Where A is the control absorbance (the measurement of DPPH solution without extract), and B is the sample absorbance (the measurement of DPPH solution with the extract). Ascorbic acid was used as the standard.

2.3.3 Molecular Docking Study

The protein data bank (http://www.rcsb.org/pdb) was used to obtain the X-ray crystal structures of the water-forming NAD(P)H oxidase (PDB ID: 2CDU, 1.80 Å resolution) and the Escherichia coli DHPR/NADH complex (PDB ID: 1DRU, 2.20 Å resolution) (Lountos et al., 2006; Alnedhary et al., 2025). These protein structures were prepared for docking using the Molecular Operating Environment (MOE). First, any unwanted atoms, molecules, chains, or ligands were removed using MOE's sequence editor window (2CDU: water molecules and the co-crystallized ligands ADP and FAD were eliminated; 1DRU: water molecules and the NAD ligand were eliminated). The second phase involved adding polar hydrogen atoms. Finally, Amber12 EHT was employed to minimize energy with an RMS of 0.1 kcal/mol/Å². We typed and modified 3936 atoms (1DRU) and 6943 atoms (2CDU); the ligand pocket of 1DRU has 154 amino acids, while the largest pocket of 2CDU has 229 amino acids. Following ChemDraw's design of the ligands' 2D structures, MOE software

was used to build the 3D structures while accounting for protonation, partial charges, and energy minimization (Arwa et al., 2022; Ali et al., 2022). Finally, a database file with the ligands was prepared and saved for docking. Docking was performed with certain parameters (rescoring function 1 and rescoring function 2: London dG; placement: triangle matcher; retain: 2; and refinement: force field) to detect and examine the ligand–protein interaction. Based on a compound's overall characteristics, such as energy, H-bond count, and location, it was selected for visualization.

3. Results and Discussion

3.1. Fourier-Transform Infrared (FTIR)

The methanolic extract of *Corchorus olitorius* leaves exhibited a characteristic band at 2931.60 cm^{-1} indicating the presence of alkane (C–H stretch). The band at 3344.06 cm^{-1} was assigned to C–H stretch of alkynes (RC≡CR), –OH dimer of carboxylic acid (RCOOH, C=C–CO–OH), Ar–OH (H-bonded phenols), and N–H stretch of amines (R_2NH). The band at 2099.21 cm^{-1} referred to N=C of RN=C=S. The band at 1632.42 cm^{-1} was due to N–H out of plane and NH_2 in-plane bending of RNH_2. The band at 1517.34 cm^{-1} referred to N–O of aromatic nitro compounds, N=O of nitroso compounds, and N–O asymmetric stretch of nitro compounds. The band at 1440.91 cm^{-1} was due to S=O of sulfate esters and Ar–C–C stretch of aromatic compounds in the ring. The band at 1364.31 cm^{-1} was due to S=O of sulfonyl chloride, S=O of sulfate ester, and C–H rock of alkane; the band at 1364.76 cm^{-1} could be due to S=O of sulfonyl chloride, S=O of sulfate esters, and C–H rock. The band at 1264.37 cm^{-1} referred to C–F stretch of alkyl halides, N–O of aromatic amine oxide, C–O stretch of carboxylic acid (RCOOH), and C–H wag of alkyl halide ($–CH_2–X$). The band at 1199.52 cm^{-1} was assigned to C–F stretch of alkyl halides, C=S of thiocarbonyl, P–H bending of phosphine, P=O of phosphine oxide, P=O of phosphate, C–O stretch of carboxylic acid (RCOOH), C–O stretch of ester, and C–H wag of alkyl halide ($–CH_2–X$). The band at 1100.92 cm^{-1} was due to C–F stretch of alkyl halides, C–O stretch of alcohols (RCH_2OH), C–O stretch of ether (R–O–R), C=S of thiocarbonyl, P–H bending of phosphine, P=O of phosphine oxide, P=O of phosphate, C–O stretch of carboxylic acid (RCOOH), and C–O stretch of ester. The band at 1052.22 cm^{-1} was due to C–F stretch of alkyl halides, C–O stretch of alcohols (RCH_2OH), C–N stretch of amines (RNH_2, R_2NH), C=S of thiocarbonyl, S=O of sulfoxide, P–H bending of phosphine, Si–OR, C–O stretch of carboxylic acid, and C–O stretch of ester (RCOOR'). The band at 993.39 cm^{-1} may be due to =CH out of plane of alkenes, P–H bending of phosphine, and P–OR of esters. The band at 920.76 cm^{-1} was due to P–OR of esters and O–H bend of carboxylic acids (RCO–OH). The bands at 624.99 and 612.49 cm^{-1} were due to ≡C–H bend of alkynes (RC≡CH) and C–Br stretch of alkyl halide, as shown in Figure 1.

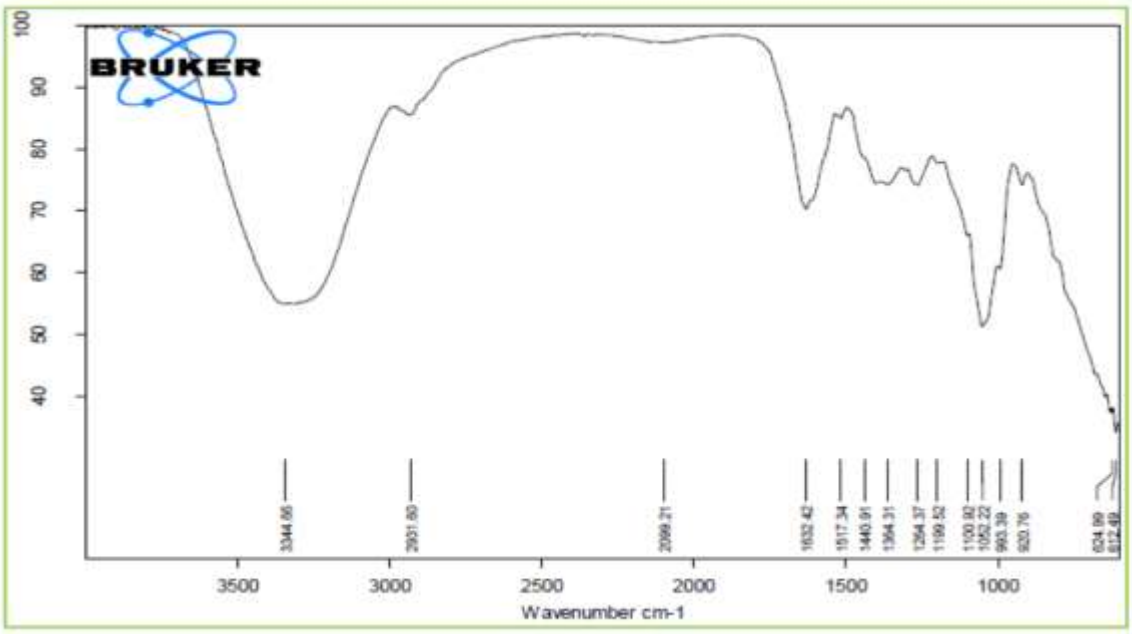

Figure 1. Fourier-transform infrared (FTIR) spectrum of methanol extract.

3.2. LC-MS Analysis

Corchorus olitorius methanol extract was analyzed using HR-LCMS, which identified ninety-six compounds. Fifty-four compounds (positive ionization mode) and forty-two (negative ionization mode) were identified based on retention time, mass, and molecular formula, as shown in Tables 1 and 2. In the chromatograms, Figures 2 and 3 depict the approximate concentrations of the various components present in *Corchorus olitorius* that elute following the retention time. The height of the peak was used to calculate the relative concentration of the bioactive substances found in the plant extract. The compounds that were eluted at different times are examined by the mass spectrometer to ascertain the makeup and structure of the compounds. Positive and negative ion modalities were used to identify phytochemicals with proton-donor and proton-acceptor properties. The foundation of a fragment at a particular mass ion was predicted to be phytocompounds, and a database search supported this prediction. The principal substances identified related to several secondary metabolite groups, such as alkaloids, terpenes, steroids, Vitamin B2 (Riboflavin), sesquiterpenoids, flavones, diterpenoids, flavonoids, fatty acids, polyphenols, steroidal alkaloids, and hydroquinone, based on the study of HR-LCMS and a comprehensive literature search. Some of these compounds have been reported to have biological activities, such as cryptochlorogenic acid (antioxidant and anti-inflammatory; Zhao et al., 2020) and quercetin (antioxidant and anti-inflammatory; Qi et al., 2022). Alshabi et al. (2022) reported the presence of 5-(3-furan-2-yl-acryloyl)-2,2-dimethyl-4,6-dioxo-cyclohexanecarboxylic acid methyl ester and 1-(8-quinolinyl)-beta-carboline as major compounds in the methanolic extract of the whole plant by using LC-MS analysis.

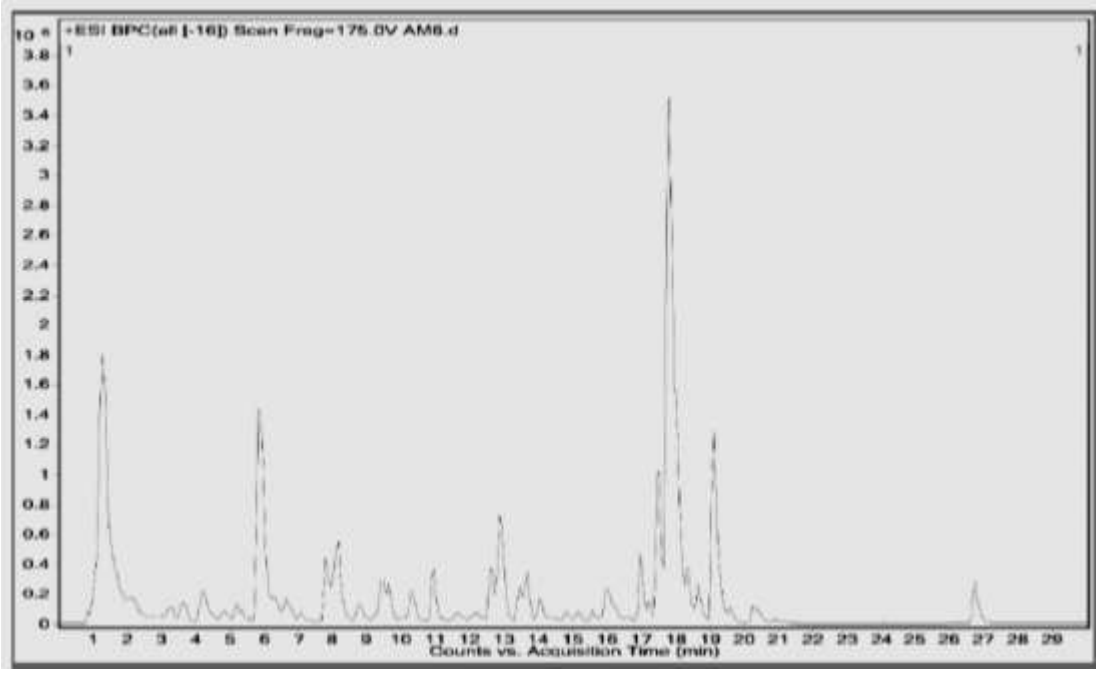

Figure 2. HR-LCMS chromatogram of extract, positive ionization mode

Table 1. List of phytochemicals identified from methanolic extract of leaves of *Corchorus olitorius* using HR-LC-MS, positive ionization mode**.**

No	Name	Formula	Mass	RT	*m/z*
1	Dihydrocaffeic acid 3-O-glucuronide	$C_{15}H_{18}O_{10}$	358.088	1.12	381.078
2	Retronecine	$C_8H_{13}NO_2$	155.094	1.565	156.102
3	Prolyl-Arginine	$C_{11}H_{21}N_5O_3$	271.16	1.568	294.154
4	Ketotifen	$C_{19}H_{19}NOS$	309.12	1.8	310.127
5	Hydroxyatrazine	$C_8H_{15}N_5O$	197.187	2.452	220.117
6	Tetrahydropentoxyline	$C_{17}H_{22}N_2O_7$	366.14	3.073	367.148
7	5,5-Diisopropyl-2,2'- dimethyl biphenyl-3,3',4,4'-tetrone	$C_{20}H_{22}O_4$	326.149	3.14	349.138
8	4,7-Dihydroxy-2H-1- benzopyran-2-one	$C_9H_6O_4$	178.02	3.876	179.033
9	Cryptochlorogenic acid	$C_{16}H_{18}O_9$	354.09	4.142	355.101
10	Valyl-Tyrosine	$C_{14}H_{20}N_2O_4$	280.14	4.214	303.133
11	3-buten-2-one 1-(2,3,6- trimethyl phenyl)	$C_{13}H_{16}O$	188.11	4.708	189.127
12	1,4,5-Naphthalenetriol	$C_{10}H_8O_3$	176.04	5.233	177.054
13	Quercetin	$C_{15}H_{10}O_7$	302.04	5.795	303.049
14	Myricetin 7- rhamnoside	$C_{21}H_{20}O_{12}$	464.094	5.799	465.102
15	Fabianine	$C_{14}H_{21}NO$	219.16	6.069	220.169
16	6-C-Galactosylluteolin	$C_{21}H_{20}O_{11}$	448.099	6.08	449.107
17	Hesperetin 7-O-glucuronide	$C_{23}H_{24}O_{11}$	476.13	6.237	499.122
18	Inundatine	$C_{16}H_{23}NO_2$	261.17	6.66	262.179
19	Formononetin 7-(6''- malonylglucoside)	$C_{25}H_{24}O_{12}$	516.12	6.83	517.132
20	Cucurbic acid	$C_{12}H_{20}O_3$	212.14	7.057	213.148

21	Flazine	$C_{17}H_{12}N_2O_4$	308.078	7.748	309.086
22	11H-Benz[bc]aceanthrylene	$C_{19}H_{12}$	240.09	7.831	263.080
23	trans-Resveratrol 3,5- disulfate	$C_{14}H_{12}O_9S_2$	387.996	7.905	389.003
24	Chloramphenicol 3- acetate	$C_{13}H_{14}Cl_2N_2O_6$	364.016	8.036	387.005
25	Thelephoric acid	$C_{18}H_8O_8$	352.009	8.13	375.005
26	3-tert-Butyl-5- methyl catechol	$C_1H_{16}O_2$	180.114	9.419	181.122
27	(5b,7a,12a)-(1,3- dihydro-5-nitro-1,3- di-oxo-2H-isoindoline-2- yl)methyl ester	$C_{33}H_{44}N_2O_8$	596.32	9.571	619.312
28	6beta-Fluoro-5alpha-hydroxy pregnane-3,20- dione	$C_{21}H_{31}FO_3$	350.225	10.102	351.233
29	(9Z,11E,13E,15Z)-4- Oxo-9,11,13,15- octa-decatetraenoic acid	$C_{18}H_{26}O_3$	290.187	10.41	291.195
30	(3b,20R,22R)-3,20,27- Trihydroxy-1-oxowitha- 5,24-dienolide 3- glucoside	$C_{34}H_{50}O_{11}$	634.335	10.912	635.343
31	Terminaline	$C_{23}H_{41}NO_2$	363.312	12.662	364.320
32	Gingerglycolipid A	$C_{33}H_{56}O_{14}$	676.365	12.754	699.355
33	Fluticasone propionate	$C_{25}H_{31}F_3O_5S$	500.183	12.875	501.191
34	Austinol	$C_{25}H_{30}O_8$	458.194	12.903	481.184
35	Trenbolone	$C_{18}H_{22}O_2$	270.161	12.908	293.153
36	Triamcinolone diacetate	$C_{25}H_{31}FO_8$	478.200	13.191	501.190
37	Norrubrofusarin 6-beta-gentiobioside	$C_{26}H_{30}O_{15}$	582.149	13.472	605.140
38	Linoleoyl Ethanolamide	$C_{20}H_{37}NO_2$	323.281	15.626	324.289
39	23- Acetoxysoladulcidine	$C_{29}H_{47}NO_4$	473.349	15.876	496.338
40	Phaeophorbide b	$C_{35}H_{34}N_2O_6$	606.246	16.171	607.254
41	3-Oxopregn-4-ene- 20beta-carboxalde-hyde dioxime	$C_{22}H_{34}N_2O_2$	358.264	16.235	359.272
42	Harderoporphyrin	$C_{35}H_{36}N_4O_6$	608.262	16.972	609.27
43	Lucidenic acid E2	$C_{29}H_{40}O_8$	516.274	17.018	539.264
44	Hematoporphyrin	$C_{34}H_{38}N_4O_6$	598.281	17.682	621.269
45	Endomorphin-2	$C_{32}H_{37}N_5O_5$	570.285	17.697	593.275
46	Pheophorbide a	$C_{35}H_{36}N_4O_5$	592.279	17.911	593.275
47	Pyropheophorbide a	$C_{35}H_{34}N_4O_3$	534.262	18.317	535.270
48	16beta-Hydroxysteroid	$C_{19}H_{32}O_2$	292.239	18.594	293.247
59	Demethyl-desacetyl-rifamycin S	$C_{34}H_{41}NO_{11}$	639.276	18.606	640.284
50	O-Methylsomniferine	$C_{37}H_{38}N_2O_7$	622.278	18.688	623.286
51	Euphornin	$C_{33}H_{44}O_9$	584.301	19.209	607.291
52	Propaquizafop	$C_{22}H_{22}ClN_3O_5$	443.118	19.423	466.110
53	Antimycin A1	$C_{28}H_{40}N_2O_9$	548.276	19.82	549.285
54	Pheophytin a	$C_{55}H_{74}N_4O_5$	870.562	26.689	871.570

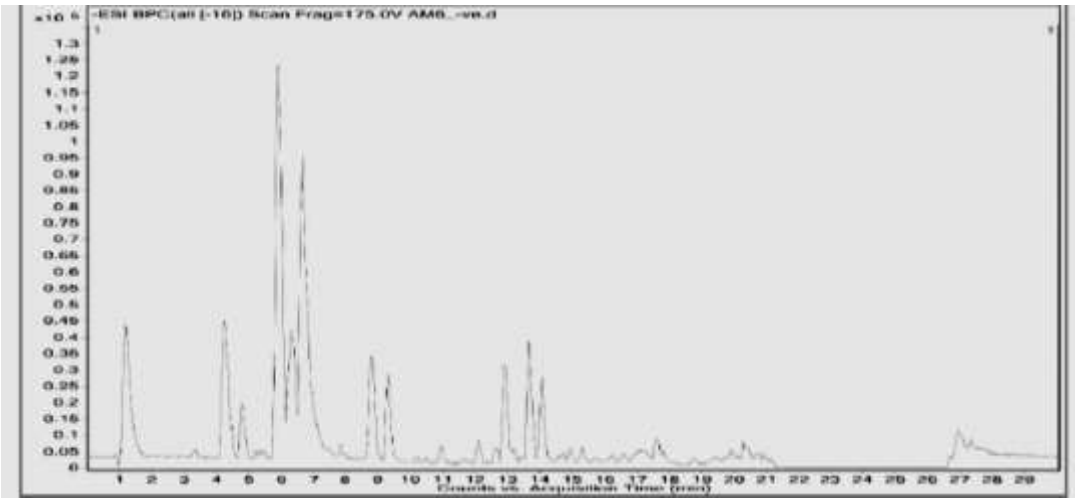

Figure 3. HR-LCMS chromatogram of extract, negative ionization mode.

Table 2. List of phytochemicals identified from the methanolic extract of leaves of *Corchorus olitorius* using HR-LC-MS, negative ionization mode.

N0	Name	Formula	Mass	RT	3.1. m/z
1	Fluorodifen	$C_{13}H_7F_3N_2O_5$	328.025	1.051	**1**
2	Chlorphoxim	$C_{12}H_{14}ClN_2O_3PS$	332.014	1.155	**377.013**
3	6"-Malonylastragalin	$C_{24}H_{22}O_{14}$	534.092	1.183	**533.085**
4	S-Methyl-3-phospho-1- thio-D-glycerate	$C_4H_9O_6PS$	215.983	1.227	**214.976**
5	Fentin acetate	$C_{20}H_{18}O_2Sn$	402.036	3.273	**447.035**
6	Fosphenytoin	$C_{16}H_{15}N_2O_6P$	362.072	4.733	**421.087**
7	Tetracenomycin A2	$C_{23}H_{18}O_8$	422.094	5.121	**421.087**
8	Digallate	$C_{14}H_{10}O_9$	322.033	5.232	**367.032**
9	Benzofenap	$C_{22}H_{20}Cl_2N_2O_3$	430.083	5.359	**429.076**
10	Di-2-propenyl pentasulfide	$C_6H_{10}S_5$	241.937	5.797	**300.952**
11	Chloralose	$C_8H_{11}Cl_3O_6$	307.961	5.8	**352.960**
12	Trisjuglone	$C_{33}H_{12}O_9$	516.044	6.221	**515.037**
13	Myricetin	$C_{22}H_{16}O_{15}S$	552.016	6.334	**551.009**
14	Riboflavin	$C_{17}H_{20}N_4O_6$	376.137	7.783	**375.131**
15	Dixanthogen	$C_6H_{10}O_2S_4$	241.956	7.847	**300.970**
16	Demeton-S-methylsulphon	$C_6H_{15}O_5PS_2$	262.008	7.887	**307.007**
17	Isomethiozin	$C_{12}H_{20}N_4OS$	268.137	8.731	**327.151**
18	L-N-(1H-Indol-3- ylacetyl) glutamic acid	$C_{15}H_{16}N_2O_5$	304.107	8.824	**363.123**
19	(1S,4R)-10- Hydroxyfenchone glucoside	$C_{16}H_{26}O_7$	330.172	9.276	**329.166**
20	7-Epiloganin tetraacetate	$C_{25}H_{34}O_{14}$	558.193	9.62	**617.207**
21	Bruceoside A	$C_{32}H_{42}O_{16}$	682.233	10.135	**727.234**
22	Methohexital	$C_{14}H_{18}N_2O_3$	262.127	10.288	**307.125**

23	Lex-lactose	$C_{32}H_{55}NO_{25}$	853.313	10.46	**471.656**
24	Gnidicin	$C_{36}H_{36}O_{10}$	628.227	10.914	**673.227**
25	Tetrahydropteroyltri-L-glutamate	$C_{24}H_{34}N_8O_{12}$	626.227	10.939	**671.226**
26	Chlorophyll c	$C_{35}H_{32}N_4O_5$	588.238	10.958	**633.237**
27	Amylopectin	$C_{30}H_{52}O_{26}$	828.282	12.09	**873.283**
28	Cemandil (O-Formylcefamandole)	$C_{19}H_{18}N_6O_6S_2$	490.070	12.905	**535.070**
29	Leucyl-Tyrosine	$C_{15}H_{22}N_2O_4$	294.154	13.075	**293.147**
30	8-Acetoxy-4'- methoxypinoresinol 4-glucoside	$C_{29}H_{36}O_{13}$	592.207	13.11	**637.208**
31	Eucommin A	$C_{27}H_{34}O_{12}$	550.202	13.451	**549.198**
32	Chlorhexidine	$C_{22}H_{30}Cl_2N_{10}$	504.200	13.809	**549.199**
33	3b,8b-Dihydroxy-6b-(3- chloro-2-hydroxy-2- methylbutanoyloxy)- 7(11)-eremophilen- 12,8-olide	$C_{20}H_{29}ClO_7$	416.152	13.955	**475.166**
34	7- Hydroxychlorophyllide a	$C_{35}H_{34}MgN_4O_6$	630.243	14.029	**689.258**
35	Prupaside	$C_{27}H_{36}O_{12}$	552.218	14.611	**551.213**
36	Halcinonide	$C_{24}H_{32}ClFO_5$	454.191	15.68	**453.183**
37	1,8- Diazacyclotetradecane- 2,9-dione	$C_{12}H_{22}N_2O_2$	226.166	16.744	**271.165**
38	Amlexanox	$C_{16}H_{14}N_2O_4$	298.095	16.832	**297.088**
39	5-Oxoavermectin "2a" aglycone	$C_{34}H_{48}O_9$	600.321	17.014	**645.321**
40	Methionyl-Alanine	$C_8H_{16}N_2O_3S$	220.088	17.301	**265.087**
41	Isoswertisin 2"-O-rhamnoside	$C_{28}H_{32}O_{14}$	592.180	17.835	**591.173**
42	Isosyringinoside	$C_{23}H_{34}O_{14}$	534.199	18.983	**579.198**

4. Biological Activities

4.1. Antibacterial Activity

MIC is defined as the lowest concentration of the antimicrobial agent that inhibits microbial growth after 24 hours of incubation (Al-Qadsy et al., 2023). The leaf extract was assessed for its antibacterial potential using the broth dilution assay. The Corchorus olitorius methanolic extract antibacterial activity study revealed that it inhibited E. coli and Pseudomonas aeruginosa growth with MICs of 100 µg/mL for ampicillin and 125 µg/mL for the extract, respectively. As shown in Table 3, the extract demonstrated more potent antibacterial activity than the standard drug ampicillin against Pseudomonas aeruginosa. The extract was found to be equally effective against both Gram-positive and Gram-negative bacteria. The various phytochemicals identified in the leaf extract may be responsible for its antimicrobial activity. These results are in agreement with earlier studies (Alrabie & Farooqui, 2019; Özdenefe et al., 2018; Namwase et al., 2021; Saifan & Makone, 2023).

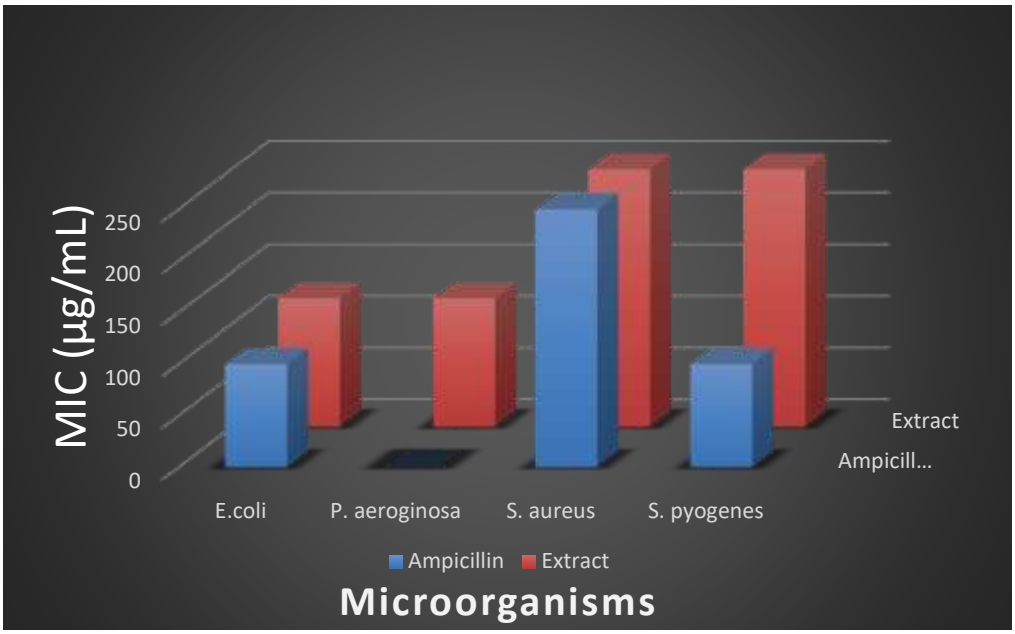

Figure 4. Minimum inhibitory concentration (MIC) (µg/mL) of extract.

Table 3. Antibacterial activity of Gram-positive and Gram-negative bacteria.

Microorganisms	*Ampicillin*	Extract
E.coli	100	125
P. aeroginosa	-	125
S. aureus	250	250
S. pyogenes	100	250

4.2. Antioxidant Activity

The DPPH radical scavenging activity of the methanol extract of plant leaves is shown in Figure 5 and Table 4. Antioxidants are believed to work by providing hydrogen, which DPPH can then use. Due to the harmful impact that free radicals play in various diseases, including cancer, radical scavenging activities are crucial for disease prevention. The DPPH free radical scavenging assay is a well-established method for evaluating the antioxidant capabilities of plant extracts. The DPPH assay involves reducing a violet-coloured DPPH solution to a yellow product, diphenylpicryl hydrazine, dependent on the concentration of the extract added. This approach has been widely utilized for predicting antioxidant activity due to the quick analysis time. The methanol extract of *Corchorus olitorius* exhibited a significant dose-dependent inhibition of DPPH activity, with 50% inhibition (IC_{50}) at a concentration of 3.24 µg/mL compared with the standard ascorbic acid (2.63 µg/mL).

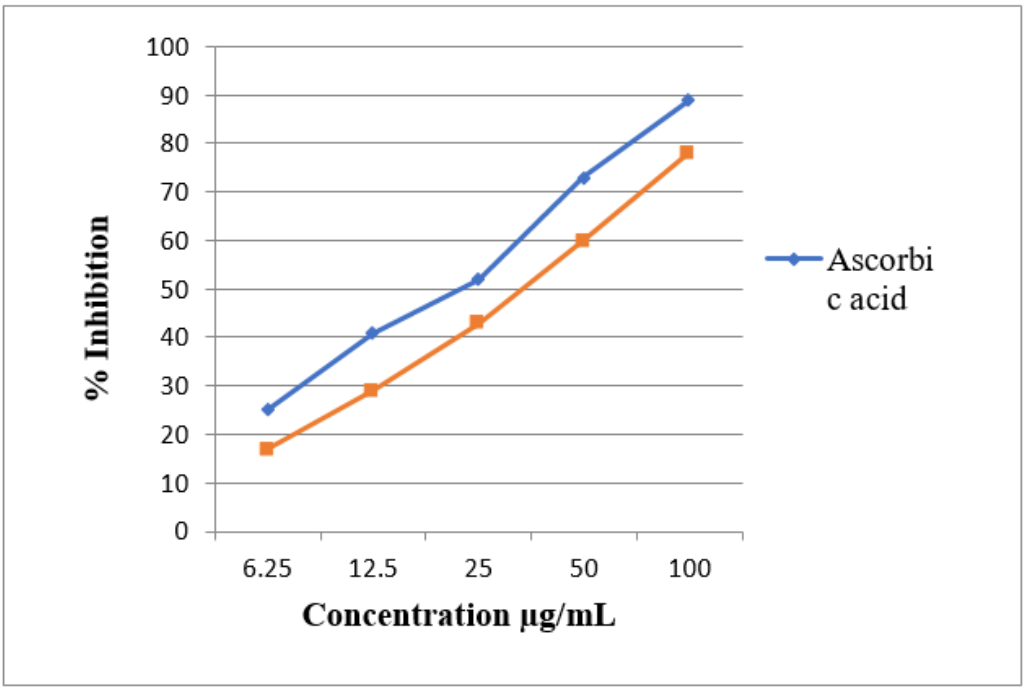

Figure 5. Percentage inhibitions of DPPH free radical activity of methanol extract of *olitorius* leaves compared with standard antioxidant ascorbic acid

Table 4. Percentage of DPPH free radical scavenging activity of *Corchorus olitorius* leaves methanolic extract

Concentration (µg/mL)	Ascorbic acid	*Corchorus olitorius*
6.25	25	17
12.5	41	29
25	52	43
50	73	60
100	89	78
IC_{50} (µg/mL)	2.63	3.24

5. Molecular Docking Study

It is helpful to conduct in silico studies to forecast the orientation and binding affinity at the receptor active site alongside in vitro antibacterial activity.

5.1. Antibacterial Activity

The molecular docking results of HR-LCMS-identified molecules (selected compounds) with the Escherichia coli DHPR/NADH complex are shown in Tables 5 and 6. Among them, the compound tetrahydropteroyltri-L-glutamate (negative ionization mode) and formononetin 7-(6"-malonylglucoside) (positive ionization mode) showed better docking efficiency with the Escherichia coli DHPR/NADH complex, with docking scores of −8.76 kcal/mol and −7.40 kcal/mol, respectively. As shown in Figure 6, tetrahydropteroyltri-L-glutamate formed seven hydrogen bonds with amino acid residues at the active site of 1DRU and seven ionic bonds. In comparison,

formononetin 7-(6"-malonylglucoside) formed only one hydrogen bond and two ionic bonds, as shown in Figure 7.

Table 5. Molecular docking results, selected compounds from the negative ionization mode.

Comp. NO.	Docking Score (Kcal/mol)	Amino acid residue	Type of bond	RMSD (Kcal/ mol)	E (Kcal/mol)	Bond Length (Å)
1	-6.02	ALA127	H-donor	1.89	-1.1	2.83
		MET17	H-donor		-0.8	3.31
2	-8.03	MET17	H-donor	1.59	-0.7	4.28
		ARG16	H-acceptor		-0.6	3.41
		HIS160	H-pi		-0.9	3.97
3	-7.51	THR104	H-acceptor	0.99	-0.5	3.30
		ARG240	H-acceptor		-1.6	3.18
		ARG240	H-acceptor		-2.4	3.18
		HIS160	H-pi		-1.0	3.75
		HIS160	H-pi		-0.8	3.83
4	-7.21	VAL217	H-donor	1.49	-3.6	3.19
		ASP165	Ionic		-3.6	3.14
5	-7.69	MET17	H-donor	1.91	-0.5	3.63
		GLN20	H-donor		-1.1	3.04
6	-8.76	GLN23	H-donor	1.78	-1.7	2.94
		THR170	H-acceptor		-1.7	3.07
		LYS163	H-acceptor		-6.0	2.96
		ARG16	H-acceptor		-3.9	2.90
		ARG16	H-acceptor		-1.7	3.07
		ARG240	H-acceptor		-1.8	3.03
		ARG240	H-acceptor		-3.4	2.93
		LYS163	Ionic		-4.7	2.96
		ARG16	Ionic		-5.2	2.90
		ARG16	Ionic		-4.0	3.07
		ARG240	Ionic		-4.3	3.03
		ARG240	Ionic		-2.4	3.37
		ARG240	Ionic		-5.0	2.93

1: 3b,8b-Dihydroxy-6b-(3-chloro-2-hydroxy-2-methylbutanoyloxy)-7(11)-eremophilen-12,8-olide; 2: 7-Epiloganin tetraacetate; 3: 8-Acetoxy-4'-methoxypinoresinol 4-glucoside; 4: Chlorhexidine; 5: Eucommin A; 6: Tetrahydropteroyltri-L-glutamate.

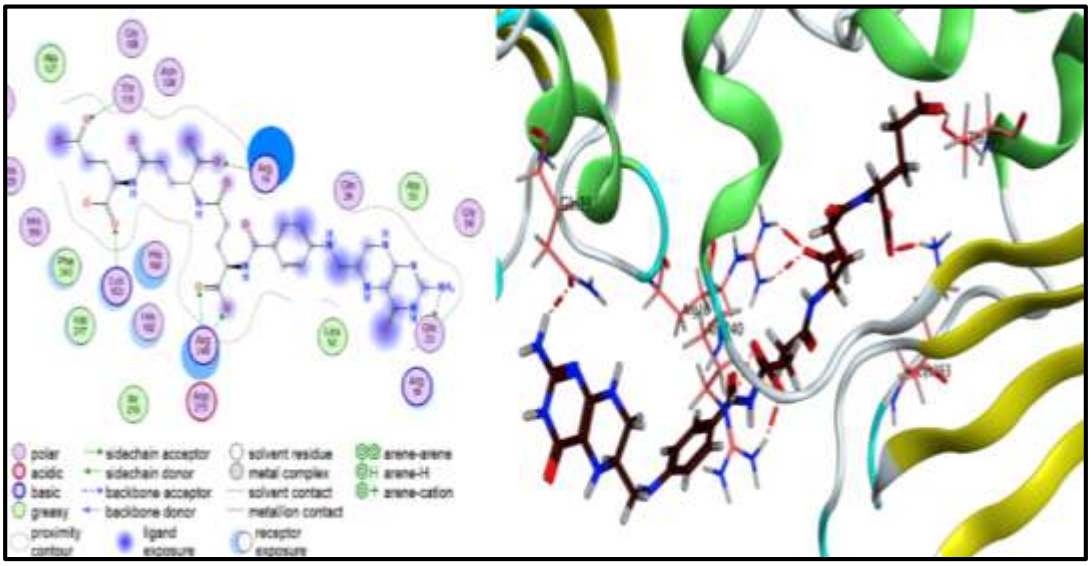

Figure 6. 2D and 3D image of tetrahydropteroyltri-L-glutamate at the active site of 1DRU.

Table 6. Molecular docking results, selected compounds from the positive ionization mode.

Comp. NO.	Docking Score (Kcal/mol)	Amino acid residue	Type of bond	RMSD (Kcal/mol)	E (Kcal/mol)	Bond Length (Å)
1	-6.04	LYS163	H-acceptor	0.78	-2.4	3.09
2	-6.42	MET17	H-donor	0.84	-1.2	3.40
		LYS163	H-acceptor		-5.1	2.93
		ARG240	H-acceptor		-2.6	3.25
3	-5.61	THR104	H-donor	1.31	-1.8	2.91
		PHE79	H-donor		-0.7	3.14
		HIS160	H-acceptor		-0.6	2.94
		ARG240	H-acceptor		-2.1	3.08
4	-5.43	MET17	H-donor	1.04	-2.1	4.16
		GLY102	H-donor		-1.8	2.90
		LYS163	H-acceptor		-4.1	2.89
		LYS163	Ionic		-5.3	2.89
5	-7.40	PHE129	H-acceptor	1.21	-2.2	3.08
		LYS163	Ionic		-4.7	2.97
		LYS163	Ionic		-4.0	3.05
6	-6.44	ASP165	H-donor	1.34	-0.7	3.32
		ASP215	H-donor		-0.5	3.27
		ARG240	H-acceptor		-3.0	2.99
		HIS160	H-pi		-1.7	3.85
		HIS160	Pi-H		-2.0	3.87
7	-6.03	PHE243	H-pi	1.12	-0.5	3.49
		HIS160	Pi-H		-0.0	3.88
8	-6.44	VAL217	H-donor	1.94	-2.0	2.90
		VAL217	H-donor		-0.9	3.08
		HIS160	H-acceptor		-1.5	3.01
		LYS163	H-acceptor		-1.4	2.91
		PHE129	H-acceptor		-5.4	3.03
		ALA127	pi-H		-1.2	3.76
	-5.79	THR170	H-donor	0.77	-0.9	2.95

9		HIS160	Pi-H		-0.7	4.70

1: 5,5-Diisopropyl-2,2'-dimethylbiphenyl-3,3',4,4'-tetrone; 2: Chloramphenicol 3-acetate; 3: Cryptochlorogenic acid; 4: Flazine; 5: Formononetin 7-(6"-malonylglucoside); 6: Myricetin 7-rhamnoside; 7: Propaquizafop; 8: Tetrahydropentoxyline; 9: Thelephoric acid.

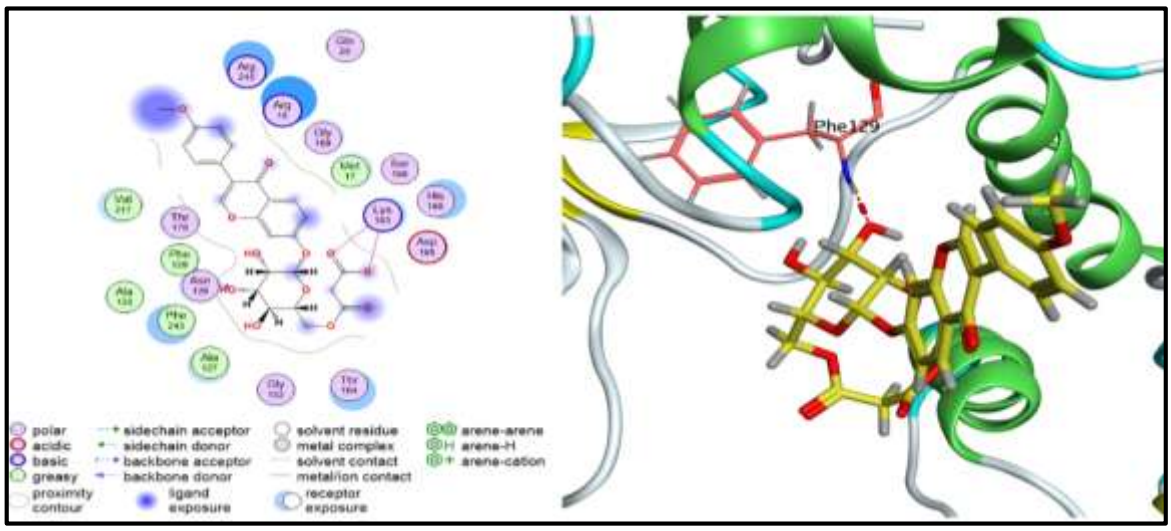

Figure 7. 2D and 3D image of Formononetin 7-(6"-malonylglucoside) at the active site of 1DRU.

5.2. Antioxidant

Our research suggests that the compounds identified may have antioxidant properties. Molecular docking research was performed to gain a better understanding of one of the potential pathways that could be causing these outcomes, which helps to support our findings. Due to its critical function in ROS production, the NADPH enzyme (PDB code: 2CDU) was selected. Research has demonstrated that this enzyme is essential for the production of reactive oxygen species (ROS), the building block of which is superoxide anion (O_2^-). To keep oxidative stress in check, medications that inhibit NADPH oxidase (NOX) are essential. The results of antioxidant molecular docking of selected compounds with the NADPH enzyme (PDB code: 2CDU) are shown in Tables 7 and 8. According to the results, tetrahydropteroyltri-L-glutamate was the most effective antioxidant. With a docking score of −9.55 kcal/mol, it formed seven hydrogen bonds, one ionic bond, and one Pi-H bond (Figure 8). Among selected compounds from the positive ionization mode, Myricetin 7-rhamnoside was the most effective antioxidant. With a docking score of −8.63 kcal/mol, it formed three hydrogen bonds with essential amino acid residues (Figure 9).

Table 7. Molecular docking results, selected compounds from the negative ionization mode.

Comp. NO.	Docking Score (Kcal/mol)	Amino acid residue	Type of bond	RMSD (Kcal/mol)	E (Kcal/mol)	Bond Length (Å)
1	-5.62	PHE245	H-acceptor	0.96	-0.5	3.13
		LYS187	H-acceptor		-7.1	2.72
2	-7.08	TYR296	H-donor	1.53	-1.6	2.86
		ASN261	H-acceptor		-1.7	3.10
		LYS187	H-acceptor		-1.4	3.18
3	-6.38	GLY329	H-donor	1.55	-2.3	2.94
		CSX42	H-donor		-1.1	3.50
		SER41	H-acceptor		-2.6	2.60
		HIS10	H-pi		-0.5	3.68
4	-8.90	GLU32	H-donor	1.87	-2.2	3.26
		GLU32	H-donor		-0.7	3.50
		THR112	H-donor		-0.9	3.54
		ALA300	H-acceptor		-0.5	3.13
		ASP282	Ionic		-0.8	3.86
		ASP282	Ionic		-0.7	3.88
		GLU32	Ionic		-2.9	3.26
		GLU32	Ionic		-1.9	3.50
		ASN135	Pi-H		-0.5	3.64
5	-8.89	CSX42	H-donor	1.49	-1.0	3.55
		GLU163	H-donor		-1.7	2.77
		CSX42	H-donor		-1.0	3.56
		CSX42	H-donor		-0.5	4.28
		ALA300	H-acceptor		-0.7	3.10
6	-9.55	ASP260	H-donor	1.93	-2.1	3.41
		ASN350	H-donor		-1.8	3.12
		TYR188	H-donor		-0.5	3.11
		PHE245	H-acceptor		-5.3	2.99
		LYS134	H-acceptor		-9.2	2.94
		ILE297	H-acceptor		-0.5	3.33
		TYR188	H-acceptor		-3.7	2.81
		LYS134	Ionic		-4.9	2.94
		LEU259	Pi-H		-0.6	4.35

1: 3b,8b-Dihydroxy-6b-(3- chloro-2-hydroxy-2- methylbutanoyloxy)- 7(11)-eremophilen-12,8-olide; 2: 7-Epiloganin tetraacetate; 3: 8-Acetoxy-4'- methoxypinoresinol 4- glucoside; 4: Chlorhexidine; 5: Eucommin A; 6: Tetrahydropteroyltri-L-glutamate

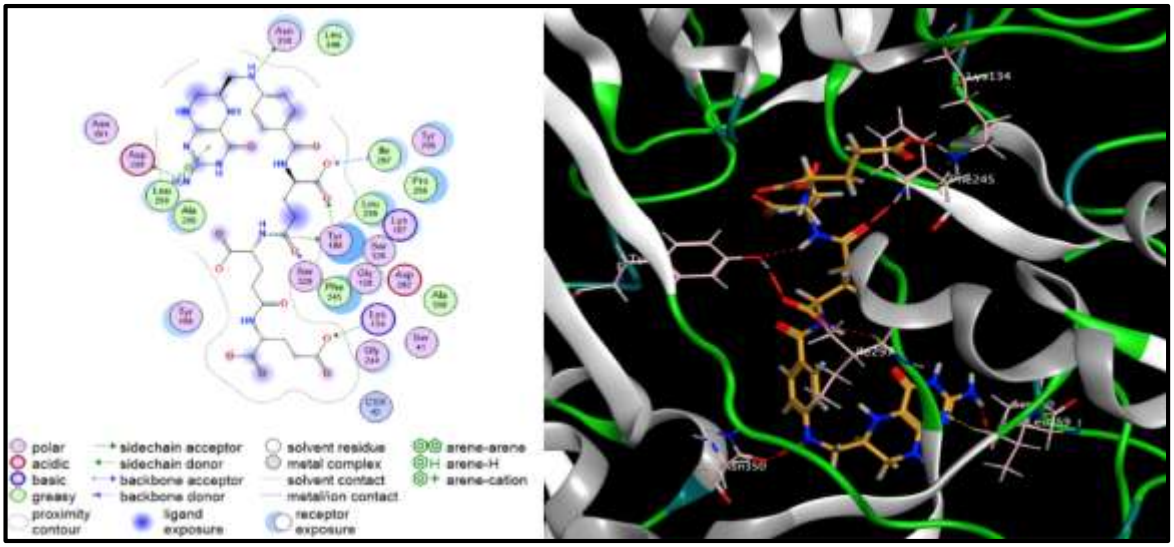

Figure 8. 2D and 3D image of tetrahydropteroyltri-L-glutamate at the active site of 2CDU.

Table 8. Molecular docking results, selected compounds from the positive ionization mode.

Comp. NO.	Docking Score (Kcal/mol)	Amino acid residue	Type of bond	RMSD (Kcal/mol)	E (Kcal/mol)	Bond Length (Å)
1	-6.56	CSX42	H-donor	0.94	-0.7	3.56
		LEU299	Pi-H		-0.6	4.01
2	-7.12	ASP282	H-donor	1.61	-0.6	3.49
		CSX42	H-donor		-0.9	3.70
		ALA11	H-acceptor		-0.9	3.05
		GLY281	H-acceptor		-0.5	3.35
		LYS134	H-acceptor		-1.4	3.21
3	-7.42	CSX42	H-donor	1.29	-0.7	3.70
		THR112	H-donor		-2.8	2.91
		LYS134	H-acceptor		-2.3	3.30
4	-5.74	TYR188	H-acceptor	1.76	-0.6	2.98
		LYS134	H-acceptor		-3.3	3.38
		LYS134	Ionic		-2.4	3.38
5	-8.46	LYS187	H-acceptor	1.95	-1.0	3.33
		LYS187	H-acceptor		-4.8	2.88
		LYS187	H-acceptor		-5.5	2.83
		LYS187	H-acceptor		-0.8	3.00
6	-8.63	MET33	H-donor	1.20	-0.6	3.11
		MET33	H-donor		-1.8	3.09
		ASP282	H-acceptor		-1.6	2.98
7	-8.17	LYS134	H-acceptor	1.59	-5.5	2.96
		SER328	H-acceptor		-0.5	3.43
		CSX42	Pi-H		-0.6	4.11
8	-6.47	CSX42	H-donor	1.83	-0.7	3.39
		PRO298	H-donor		-2.0	2.80
		LYS134	H-acceptor		-4.2	2.99
		LYS134	Ionic		-4.5	2.99

9	-7.13	THR112 THR112 LYS134	H-donor H-donor H-acceptor	0.70	-1.2 -3.8 -1.5	3.20 2.81 2.75

1: 5,5-Diisopropyl-2,2'-dimethylbiphenyl-3,3',4,4'-tetrone; 2: Chloramphenicol 3-acetate; 3: Cryptochlorogenic acid; 4: Flazine; 5: Formononetin 7-(6"-malonylglucoside); 6: Myricetin 7-rhamnoside; 7: Propaquizafop; 8: Tetrahydropentoxyline; 9: Thelephoric acid.

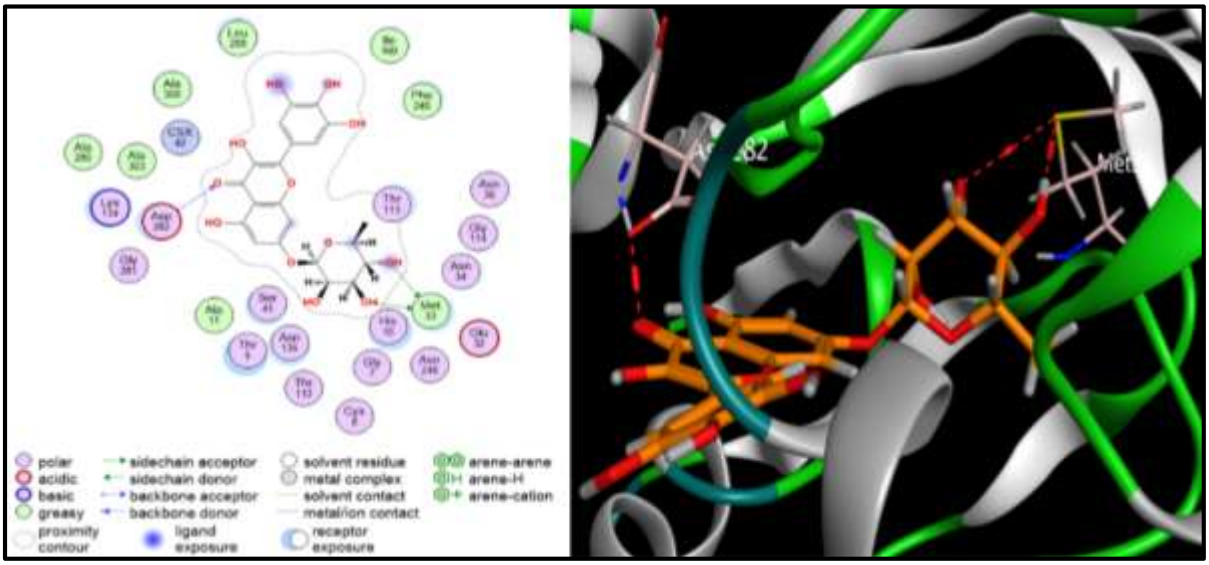

Figure 9. 2D and 3D image of Myricetin 7-rhamnoside at the active site of 2CDU.

6. Conclusion

The present study's findings demonstrated that the leaves of *Corchorus olitorius* contain a diverse array of phytochemicals that may account for the extract's purported properties. In addition, the study's presentation of key diagnostic features of *Corchorus olitorius* that may be used for identification purposes makes it a useful reference for the future.

Declaration of Competing Interest

The authors declare that they have no known competing financial interests or personal relationships that could have appeared to influence the work reported in this paper.

Acknowledgment

The authors would like to express their gratitude to Dr. Rafiuddin Naser, Head of the Botany Department at Maulana Azad College, Aurangabad, for confirming the legitimacy of the plant.

References

[1] Aziziaram, Z., Bilal, I., Zhong, Y., Mahmod, A. K., & Roshandel, M. R. (2021). Protective effects of curcumin against naproxen-induced mitochondrial dysfunction in rat kidney tissue. Cell and Molecular Biology Reports, 1(1), 23–32.

[2] Ezeonu, C. S., & Ejikeme, C. M. (2016). Qualitative and quantitative determination of phytochemical contents of indigenous Nigerian softwoods. New Journal of Science, 2016, 5601327.

[3] Elisha, I. L., Botha, F. S., McGaw, L. J., & Eloff, J. N. (2017). The antibacterial activity of extracts of nine plant species with good activity against Escherichia coli against five other bacteria and cytotoxicity of extracts. BMC Complementary and Alternative Medicine, 17(1), 1–10. https://doi.org/10.1186/s12906-017-1645-z

[4] Al-Hamoud, G. A., Fantoukh, O. I., Amina, M., Nasr, F. A., Musayeib, N. M. A., Ahmed, M. Z., & Alqahtani, A. S. (2022). Unprecedented insights on chemical and biological significance of Euphorbia cactus growing in Saudi Arabia. Plants, 11(5), 681.

[5] Sharma, T., Pandey, B., Shrestha, B. K., Koju, G. M., Thusa, R., & Karki, N. (2020). Phytochemical screening of medicinal plants and study of the effect of phytoconstituents in seed germination. Tribhuvan University Journal, 35(2), 1–11.

[6] Wadood, A., Ghufran, M., Jamal, S. B., Naeem, M., Khan, A., & Ghaffar, R. (2013). Phytochemical analysis of medicinal plants occurring in local area of Mardan. Biochemistry and Analytical Biochemistry, 2(4), 1–4.

[7] Marwa, A. M. A., Miada, F. A., Usama, R. A., & Ashraf, N. E. H. (2022). Pharmacological and phytochemical biodiversity of Corchorus olitorius. RSC Advances, 12(54), 35103–35114. https://doi.org/10.1039/d2ra07406k

[8] Kundu, A., Sarkar, D., Mandal, N. A., Sinha, M. K., & Mahapatra, B. S. (2012). A secondary phloic (bast) fiber-shy (bfs) mutant of dark jute (Corchorus olitorius L.) develops lignified fiber cells but is defective in cambial activity. Plant Growth Regulation, 67, 45–55.

[9] Giro, A., & Ferrante, A. (2016). Yield and quality of Corchorus olitorius baby leaf grown in a floating system. Journal of Horticultural Science & Biotechnology, 91, 603–610.

[10] Islam, M. M. (2013). Biochemistry, medicinal and food values of jute (Corchorus capsularis L. and C. olitorius L.) leaf: A review. International Journal of Research in Applied Science and Engineering Technology, 2, 135–144.

[11] Saifan, A. A. A., & Al-horaibi, S. A. (2021). Water extract of dragon fruit peel catalyzed synthesis of dihydropyridines by Hantzsch condensation. Journal of Chemistry and Nutritional Biochemistry, 2(1), 46–54. DOI: 10.48185/jcnb.v2i1.205

[12] Alrabie, A., Alrabie, N. A., AlSaeedy, M., Al-Adhreai, A., Al-Qadsy, I., Al-Horaibi, S. A., & Farooqui, M. (2023a). An integrative GC–MS and LC–MS metabolomics platform determination of the metabolite profile of Bombax ceiba L. root, and in silico & in vitro evaluation of its antibacterial & antidiabetic activities. Natural Product Research, 37(13), 2263–2268.

[13] Ola, B., Samreen, F., Ali, A., & Mazahar, F. (2016). Supercritical fluid extraction of Cichorium intybus (L) and its characterization. Journal of Chemical and Pharmaceutical Sciences, 9(4), 2936–2944.

[14] Samreen, F., Ola, B., Mazahar, F., & Pathan, M. A. (2018). Phytochemical and physicochemical properties of Hibiscus rosa sinensis leaves extract: A comparison between conventional and microwave-assisted extraction. European Journal of Biomedical and Pharmaceutical Sciences, 5(7), 551–559.

[15] Murshed, F., Alnedhary, A. A., AL-Hamadi, M. M., & Al-kufl, D. (2024). Development and optimization of the sample preparation method to determine the antioxidants in the yemeni almond. Sana'a University Journal of Applied Sciences and Technology, 2(3), 254-264.

[16] Alnedhary, A. A., Almaqtari, M. A., Huzaim, A. A. A., Al-kufl, D., & Al-rejal, A. A. A. (2025). Method Validation and Assessment of Total Antioxidants, Polyphenols, Flavonoids, and Vitamin C in Cultivated Mulberry in Yemen. Sana'a University Journal of Applied Sciences and Technology, 3(2), 730-739.

[17] Lountos, G. T., Jiang, R., Wellborn, W. B., Thaler, T. L., Bommarius, A. S., & Orville, A. M. (2006). The crystal structure of NAD(P)H oxidase from Lactobacillus sanfranciscensis: Insights into the conversion of O_2 into two water molecules by the flavoenzyme. Biochemistry, 45(32), 9648–9659.

[18] Alrabie, A., Al-Rabie, N. A., Al Saeedy, M., Al Adhreai, A., Al-Qadsy, I., & Farooqui, M. (2023b). Martynia annua safety and efficacy: Heavy metal profile, in silico and in vitro approaches on antibacterial and antidiabetic activities. Natural Product Research, 37(6), 1016–1022.

[19] Arwa, A. A., ALSaeedy, M., Alrabie, A., Al-Qadsy, I., Dawbaa, S., Alaizeri, Z. M., & Farooqui, M. (2022). Design and synthesis of novel enantiopure bis(5-isoxazolidine) derivatives: Insights into their antioxidant and antimicrobial potential via in silico drug-likeness, pharmacokinetic, medicinal chemistry properties, and molecular docking studies. Heliyon, 8(6).

[20] Ali, A., Arwa, A., Inas, A., Vidya, P., & Mazahar, F. (2022). Phytochemical screening, GC-MS analysis, molecular docking study, and evaluation of antioxidant and antimicrobial activity of Sapindus emarginatus seed kernel. Research Journal of Pharmacy and Technology, 15(5), 2117–2121. https://doi.org/10.52711/0974-360X.2022.00351

[21] Zhao, X. L., Yu, L., Zhang, S. D., Ping, K., Ni, H. Y., Qin, X. Y., & Fu, Y. J. (2020). Cryptochlorogenic acid attenuates LPS-induced inflammatory response and oxidative stress via upregulation of the Nrf2/HO-1 signaling pathway in RAW 264.7 macrophages. International Immunopharmacology, 83, 106436.

[22] Qi, W., Qi, W., Xiong, D., & Long, M. (2022). Quercetin: Its antioxidant mechanism, antibacterial properties and potential application in prevention and control of toxipathy. Molecules, 27(19), 6545.

[23] Alshabi, A. M., Alkahtani, S. A., Shaikh, I. A., Orabi, M. A., Abdel-Wahab, B. A., Walbi, I. A., & Asdaq, S. M. B. (2022). Phytochemicals from Corchorus olitorius methanolic extract induce apoptotic cell death via activation of caspase-3, anti-Bcl-2 activity, and DNA degradation in breast and lung cancer cell lines. Journal of King Saud University–Science, 34(7), 102238.

[24] Alrabie, A., & Farooqui, M. (2019). Gas chromatography-mass spectrometry analysis, inductively coupled plasma mass spectrometry investigation, and antimicrobial screening of Caesalpinia bonducella. GAS, 12(4).

[25] Özdenefe, M. S., Muhammed, A., Süer, K., Güler, E., & Takçı, H. A. M. (2018). Determination of antimicrobial activity of Corchorus olitorius leaf extracts. Cyprus Journal of Medical Sciences, 3(3), 159–163. https://doi.org/10.5152/cjms.2018.623

[26] Namwase, H., Najjuka, F., & Bbosa, G. (2021). Anti-bacterial activity of Corchorus olitorius L. and Acmella caulirhiza Del. on Streptococcus mutans, a cariogenic bacterium. African Health Sciences, 21(4), 1685–1691. https://doi.org/10.4314/ahs.v21i4.23

[27] Saifan, A. A. A., & Makone, S. S. (2023). Novel and efficient synthesis of lithium crown ether metal–organic framework nanoparticles (15C5-Li MOF@Bi_2O_3@TiO_2 NPs): Characterization and evaluation of its in vitro antibacterial studies: inorganic Chemistry Communications, 155, 110946. https://doi.org/10.1016/j.inoche.2023.110946

[28] Saifan, A. A. A., Hussein, F. A., Othman, A. A., Al Ans, S. A. M., Tazeen, N., Alhadlaq, H. A., & Makone, S. S. (2024). Synthesis and antibacterial evaluation of 2-phenyl-1H-benzo[d]imidazole derivatives using novel 18C6-FeMOF@Pb_2O_3@TiO_2 nanocatalyst. Inorganic Chemistry Communications, 113395. https://doi.org/10.1016/j.inoche.2024.113395